Supplemental Information

Dual-Function Thiourea for Photochemical Recovery of Precious Metals in Fe(III)-Oxalate Based System

Guangbing Liang, Hui Wang, Zhenping Qu*

Key Laboratory of Industrial Ecology and Environmental Engineering (Ministry of Education, China), School of Environmental Science and Technology, Dalian University of Technology, Dalian, 116024, China

* Corresponding author. *quzhenping@dlut.edu.cn* (Z.P. Qu)

EXPERIMENTAL SECTION

Materials and Reagents. Spent Pt-/Pd-containing catalysts used in this work were obtained from chemical industries. Deactivated Au-containing catalyst was obtained after lab test. All the catalysts were scrapped (Loss on ignition, LOI >5 wt.%), and they were used in the form of powder (60 meshes) throughout the experiment. Iron oxide (Fe_2O_3, ≥99.0%), cerium nitrate hexahydrate ($Ce(NO_3)_3·6H_2O$, ≥99.0%), oxalic acid dihydrate ($H_2C_2O_4·2H_2O$, ≥99.5%), thiourea (CH_4N_2S, ≥99.0%), *tert*-butyl alcohol ($C_4H_{10}O$, ≥99.5%), methanol (CH_3OH, ≥99.5%), sodium chloride (NaCl, ≥99.5%), urea (CH_4N_2O, ≥99.0%), ammonium sulfate ($(NH_4)_2SO_4$, ≥99.0%), ammonium persulfate ($(NH_4)_2S_2O_8$, ≥98.0%), and thioacetamide (C_2H_5NS, ≥99.0%) of analytical grade and were purchased from Sinopharm Chemical Reagent Co., Ltd. Chloroplatinic acid hydrate ($H_2PtCl_6·H_2O$, ≥99.0%), Gold chloride hydrate ($HAuCl_4·H_2O$, ≥99.0%), Ammonium tetrachloropalladate ($(NH_4)_2PdCl_4$, ≥99.0%), Ammonium thiosulfate ($(NH_4)_2S_2O_3$, 98%) and *p*-Benzoquinone ($C_6H_4O_2$, 99%) and 5,5-dimethyl-1-pyrroline-N-oxide ($C_7H_{12}N_2O$, 97%) were purchased from Aladdin Chemical Reagent Co., Ltd.

Photocatalytic Dissolution of Au, Pt, and Pd

1. Screening Experiments for Sulfide Ligands

Some sulfides, such as ammonium sulfate, ammonium thiosulfate, ammonium persulfate, thioacetamide, and thiourea, were used as ligand for photochemical dissolution in FOC-based system. In these lixiviants, the volume ratio of parent Fe(III)-oxalate addition (The concentration of parent FOC was approximately 0.1 $mol·L^{-1}$ detected by ICP-OES.) was 50 vol.% (~0.05 $mol·L^{-1}$), and the concentration of sulfides was 60 $g·L^{-1}$. In the dissolution experiments, 50 mL FOC-sulfide lixiviants was mixed with 0.05 g Au/CeZr, 0.5 g Pt/CM, and 0.5 g Pd/Al_2O_3 catalyst powders to

photochemical reaction for 4 hours, respectively. To investigate the effect of thiocarbonyl group, the comparison study of FOC-urea lixiviant was carried out, and the experimental conditions are the same as the aforementioned FOC-sulfide lixiviant.

2. Optimal Conditions for Single Precious Metal Photochemical Dissolution

The volume ratio of parent Fe(III)-oxalate addition, thiourea concentration in the lixiviant, solid-to-liquid ratio of PMs-containing catalysts, and the dissolution time were investigated in sequence.

For the single-factor test of addition amount of parent Fe(III)-oxalate, 0.05 g Au/CeZr, 0.5 g Pt/CM, or 0.5 g Pd/Al_2O_3 catalyst powders were put into 50 mL lixiviant to photochemically dissolve for 4 h, respectively. The thiourea concentration was 60 $g \cdot L^{-1}$ in the lixiviant, and the addition amounts of FOC solution were ranged into 0 vol.% (0 $mol \cdot L^{-1}$), 25 vol.% (~0.02 $mol \cdot L^{-1}$), 50 vol.% (~0.05 $mol \cdot L^{-1}$), 75 vol.% (~0.07 $mol \cdot L^{-1}$), and 100 vol.% (~0.1 $mol \cdot L^{-1}$), respectively.

For the single-factor test of thiourea concentration in the lixiviant, the component was changed from 20 $g \cdot L^{-1}$ to 100 $g \cdot L^{-1}$. The usage of spent catalysts was still 0.05 g Au/CeZr, 0.5 g Pt/CM, or 0.5 g Pd/Al_2O_3 catalyst powders in 50 mL lixiviant, reaction for 4 h. While the addition amount of FOC was 25 vol.% in Au dissolution experiment, and was 50 vol.% in Pt or Pd dissolution experiment.

For the single-factor test of solid-to-liquid (S-L) ratio of PMs-containing catalysts and lixiviant, the usages of spent catalysts were quite different due to their different contents of PMs. In the experiment of Au dissolution, 50 mL lixiviant containing 25 vol.% FOC and 40 $g \cdot L^{-1}$ thiourea was used to react for 4 h. The usages of Au/CeZr powder were 0.01 g (S-L=0.2 $mg \cdot mL^{-1}$), 0.02 g (S-L=0.4 $mg \cdot mL^{-1}$), 0.03 g (S-L=0.6 $mg \cdot mL^{-1}$), 0.04 g (S-L=0.8 $mg \cdot mL^{-1}$), and 0.05 g (S-L=1.0 $mg \cdot mL^{-1}$), respectively. In the experiment of Pt dissolution, 50 mL lixiviant containing 50 vol.% FOC and 60 $g \cdot L^{-1}$

thiourea was used to react for 4 h. The usages of Pt/CM powder were 0.1 g (S-L=2 $mg \cdot mL^{-1}$), 0.2 g (S-L=4 $mg \cdot mL^{-1}$), 0.3 g (S-L=6 $mg \cdot mL^{-1}$), 0.4 g (S-L=8 $mg \cdot mL^{-1}$), and 0.5 g (S-L=10 $mg \cdot mL^{-1}$), respectively. In the experiment of Pd dissolution, 50 mL lixiviant containing 50 vol.% FOC and 60 $g \cdot L^{-1}$ thiourea was used to react for 4 h. The usages of Pd/Al_2O_3 powder were 0.5 g (S-L=10 $mg \cdot mL^{-1}$), 0.6 g (S-L=12 $mg \cdot mL^{-1}$), 0.7 g (S-L=14 $mg \cdot mL^{-1}$), 0.8 g (S-L=16 $mg \cdot mL^{-1}$), and 0.9 g (S-L=18 $mg \cdot mL^{-1}$), respectively. Herein, the PM dissolution efficiency (η) was calculated in accordance with **eq. S1**.

$$\eta_i\ (\%) = \frac{V_i \times C_i}{\omega_i \times m_i} \times 100 \tag{S1}$$

Where *i* represents the PMs of gold, platinum and palladium, respectively. ω is the mass concentration of PMs in the wastes, $mg \cdot kg^{-1}$. *m* is the mass of waste addition, kg. *V* is the volume of PM-containing lixivium, L. *C* is the PM concentration in the lixivium, $mg \cdot L^{-1}$.

Apparently, the dissolution rate of *r* was necessary to be introduced to describe the dissolution amount of PMs for per hour in the whole process when the PMs were dissolved from the secondary resources under the optimal conditions, as followed in the **eq. S2**.

$$r_i = \frac{M_i}{t} \tag{S2}$$

Where *M* is the mass of PMs in the leaching solution under the optimal condition, mg. *t* is the reaction time, h.

3. Photochemical Dissolution Performance for Blended Precious Metals

Considering about the dissolution priority of PMs in a blended feeding, so it was necessary to discuss the co-dissolution performance for PMs recovery. In this section, the FOC-T lixiviant contained 50 vol.% FOC and 60 $g \cdot L^{-1}$ thiourea. The changes of

photochemical dissolution efficiency with 0.17 g Pt/CM (~0.1 mg Pt) + 0.24 g Pd/Al_2O_3 (~0.1 mg Pd) powder or 0.01 g Au/CeZr (~0.1 mg Au) + 0.24 g Pd/Al_2O_3 (~0.1 mg Pd) powder in 100 mL FOC-T lixiviant were recorded within 6 hours. Then, the dissolution efficiencies of lixiviant mixed with 0.17 g Pt/CM (~0.1 mg Pt) + 0.47 g Pd/Al_2O_3 (~0.2 mg Pd) powder, 0.34 g Pt/CM (~0.2 mg Pt) + 0.24 g Pd/Al_2O_3 (~0.1 mg Pd) powder, and 0.34 g Pt/CM (~0.2 mg Pt) + 0.47 g Pd/Al_2O_3 (~0.2 mg Pd) powder were investigated after the photochemical dissolution for 5 h. Meanwhile, 0.01 g Au/CeZr (~0.1 mg Au) + 0.47 g Pd/Al_2O_3 (~0.2 mg Pd) powder, 0.02 g Au/CeZr (~0.2 mg Au) + 0.24 g Pd/Al_2O_3 (~0.1 mg Pd) powder, and 0.02 g Au/CeZr (~0.2 mg Au) + 0.47 g Pd/Al_2O_3 (~0.2 mg Pd) powder were also mixed with FOC-T lixiviant to react for 4 h to obtain the dissolution performance for blended precious metals of Au and Pd.

4. Kinetics Rate Calculation and Additional Experiments of Single Precious Metal

To make sure the comparability among dissolution kinetics rates, the input amount of single PMs should be consistent. 0.51 g Pt/CM (~0.3 mg Pt), 0.71 g Pd/Al_2O_3 (~0.3 mg Pd), or 0.03 g Au/CeZr (~0.3 mg Au) powders was added into 50 mL FOC-T lixiviant to react within 1 h, respectively. All the lixiviants contained 50 vol.% FOC and 60 g·L^{-1} thiourea. Herein, the chemical reaction control model (**eq. S3**) and the diffusion control model (**eq. S4**) were used to simulate the dissolution kinetics of PMs and evaluate the dissolution rate during the photocatalytic dissolution[1].

$$1-(1-x_i)^{\frac{1}{3}} = k_1 t \tag{S3}$$

$$1-\frac{2}{3}x_i-(1-x_i)^{\frac{2}{3}} = k_2 t \tag{S4}$$

Where x denotes the PMs dissolution efficiency, %. k_1 and k_2 are the reaction rate constants of the two models, respectively, h^{-1}. t is the reaction time, h.

When it came to study on the effect of FOC and thiourea in FOC-T system, the

optimal dissolution conditions were applied for Au, Pt or Pd recovery according to section S1. The photochemical dissolution efficiencies of Au, Pt, and Pd were investigated with the lixiviants of bare FOC under darkness or irradiation, bare thiourea under darkness or irradiation, and FOC-T under darkness. Additionally, the thiourea ligand was replaced by NaCl to determine the differences during photochemical dissolution of PMs. The concentration of ligand was still 40 $g \cdot L^{-1}$ for Au dissolution, 60 $g \cdot L^{-1}$ for Pt and Pd dissolution. Then, photochemical liquid oxidant of FOC was changed into the TiO_2 (P25) or g-C_3N_4 photocatalysts, and the total volume was 50 mL containing 50 mg solid catalysts and a certain concentration of thiourea in deionized water to dissolve PMs for a period of irradiation. It evaluated the differences of photochemical dissolution performance among different ligands and photochemical oxidants for the PMs recovery.

Computational Methods

A plane wave (PW) energy cutoff of 450 Ry was employed for the calculation of electrostatic energy terms, while a relative cutoff of 50 Ry was utilized for Gaussian mapping on multigrid levels. the adsorption energy (ΔE_{ads}) between the thiourea molecule and PMs were defined as followed in **eq. S5**.

$$\Delta E_{ad} = E_{Total}^{Thio-M} - E_{Frag}^{Thio} - E_{atom}^{M} \quad \text{(S5)}$$

Where the *M* represents the PMs, i.e. Au, Pt, and Pd. *Thio-M* denotes the adsorbed states between thiourea and PMs. E_{Total}^{Thio-M} is the total energies of adsorbed states. E_{Frag}^{Thio} is the energy of thiourea fragment. E_{atom}^{M} is the energy of PM atoms.

The formation energy (ΔE_f) of thiourea oxidization in FOC-T and TiO_2-thiourea systems were given out as followed in **eq. S6**.

$$\Delta E_f = E_{Sol}^{(Thio)*O} - E_{Sol}^{Thio} - E_{Sol}^{*O} \quad \text{(S6)}$$

Where *(Thio)*O* denotes the oxidization product of thiourea. *Sol* is the liquid phase compositions of FOC or H_2O (TiO_2). condition PMs-Thiourea complexes. $E_{Sol}^{(Thio)*O}$ is the total energy of thiourea oxidization in FOC or H_2O (TiO_2). E_{Sol}^{Thio} is the energy of an isolated thiourea molecule in FOC or H_2O (TiO_2), and E_{Sol}^{*O} is the energy of reactive oxygen atom in FOC or H_2O (TiO_2).

Characterization.

All the spent catalyst powders were dissolved in the aqua regia solution to determine the contents of precious metals by inductively coupled plasma−optical emission spectrometry (ICP-OES). Fourier transform infrared spectroscopy (FTIR) was used to estimate the chemical structures in range from 4000 cm^{-1}-400 cm^{-1} with a resolution of 4 cm^{-1}. X-ray photoelectron spectroscopy (XPS) was used to analyze the valence bands related to Au 4f, Pt 4f and Pd 3d of PMs, and S 2p in the PMs(Thio). XPS was equipped with an Al Ka anode monochromatic X-ray source (1486.6 eV), whose binding energy values were regulated with referenced to the adventitious C 1s position at 284.8 eV. Confocal laser Raman spectrometer equipped with 532 nm (5 mW) wave-length laser and the data was collected by corresponding software (Wire) in the Raman shift from 200 to 2000 cm^{-1}. The Raman shift was calibrated to 520 cm^{-1} using a Si wafer. The crystal phases of samples were measured using an X-ray diffraction (XRD) equipped with Cu Kα radiation source (λ = 1.54 Å) from 10° to 60° in 2θ range with 0.020° step interval and 2 sec $step^{-1}$ counter time. The UV-vis spectrophotometer from 190 to 900 nm was recorded with a UV2600 spectrophotometer. FTIR, XPS, Raman, and UV-vis analysis were applied for the final product powder obtained after the washing and drying from the product powder. Electron paramagnetic resonance (EPR) was used to qualitatively analyze the formation

of ˙OH, $SO_4^{\bullet-}$ and $O_2^{\bullet-}$. EPR spectra were measured by the trapping agent of DMPO at room temperature with a center field of 3500 G, resonance frequency of 9.88 GHz, microwave power of 1.65 mW, modulation frequency of 100 kHz, sweep width of 200 G. Laser flash photolysis (LFP) spectrometer equipped with LP920-KS system was used to detect the generation of active radicals and evaluate their lifetime in the solution under the irradiation. $[Fe_2(C_2O_4)_3] \approx 1.83\times10^{-3}$ M, $[H_2C_2O_4] \approx 2.62\times10^{-2}$ M. The pump laser is a Nd:YAG laser (10 Hz rep rate) operating at 355 nm with ulse duration 7 ns. The system is normally operated at 1 Hz. The probe is a 450 W pulsed Xenon arc lamp for kinetic and spectral measurements. The spectral range is 200-850 nm, and the temporal resolution is 50 ns.

Catalyst Preparation and Catalytic Activity Measurement for Toluene Degradation

1. PMs/CeO_2 Catalysts Prepared by Commercial Reagents and Recovered Lixiviums

CeO_2 nanocubes were synthesized by a hydrothermal method at 180 °C for 24 h under autogenous pressure and static conditions as mentioned by Sun et al.[2] The recovered Au, Pt, and Pd-containing lixiviums were approximately concentrated to 0.1 g/L (PMs contents) detected by ICP-OES. Then, a total 0.4 g of CeO_2 nanocube was dispersed into the 20 mL PMs-containing lixivium and stirred at room temperature for 1 h. 2 mL $NaBH_4$ and NaOH mixing solution ($NaBH_4$/NaOH = 1/5, molar ratio) was added to the suspension mentioned above, and the suspension was then stirred for another 1 h. Finally, the samples were washed with deionized water four times and ethanol once, and dried in the oven at 80 °C for 12 h, as denoted PMs (Pt, Pd, Au)/CeO_2-R. At the same time, the commercial PMs reagents were also prepared into 0.1 g/L solution, the follow-up method was the same as aforementioned synthesis procedure. The catalysts are denoted as PMs (Pt, Pd, Au)/CeO_2-C.

2. Catalytic Activity Measurement of Toluene Oxidation Degradation

The catalytic activity of toluene oxidation was performed at atmospheric pressure in a tubular fixed-bed reactor system of 4 mm inner diameter. The reaction mixtures were flowed into 0.1 g (40-60 meshes) catalysts with a weight hourly space velocity (WHSV) of 60000 $mL \cdot g^{-1} \cdot h^{-1}$. The component of the feed gases was 1000 ppm toluene, 20% O_2/N_2, and the total flow rate was 100 mL/min. The 1000 ppm toluene in the gas mixture was produced through a bottle filled with bare toluene by using an N_2 bubbler. All reaction gas lines were heated to 100 ^oC by a heating belt to prevent toluene condensation on the tube walls. The reactants and products were in-situ analyzed online by using a gas chromatograph (Shimadzu, GC-2014) equipped with a flame ionization detector (FID) and thermal conductivity detector (TCD). The conversion of toluene was calculated according to **eq. S7.**

$$X_{Toluene} = \frac{[Toluene]_{in} - [Toluene]_{out}}{[Toluene]_{in}} \times 100\% \quad \text{(S7)}$$

where $[Toluene]_{in}$ represents the inlet toluene concentration, and $[Toluene]_{out}$ is the outlet toluene concentration.

Structural Parameters of Adsorption Model with Thiourea Molecule and Au

Tv_1:	9.989800	0.000000	0.000000
Tv_2:	0.000000	11.535200	0.000000
Tv_3:	0.000000	0.000000	28.598672
Au	4.79644193	1.94838087	0.74077596
Au	9.79143664	4.83113774	0.74634355
Au	1.47935392	1.94609309	3.23040732
Au	6.46533473	4.82777777	3.19746022
Au	8.14796539	1.94194515	5.64622237
Au	3.15720646	4.82758144	5.62860874
Au	4.82404135	1.91679057	8.09982856
Au	9.82388491	4.83099436	8.13154363
Au	7.29287297	0.50975260	0.74136109
Au	2.29906186	3.38838448	0.74041390
Au	3.97530845	0.50425539	3.21857234
Au	8.96907001	3.38687591	3.22197758
Au	0.65550081	0.50062480	5.65241684
Au	5.64292973	3.39132873	5.65855498
Au	7.32275496	0.49506702	8.12931065
Au	2.31591066	3.37433138	8.09596603
Au	9.79261563	1.94938766	0.76003573
Au	4.79378824	4.83011561	0.70633486
Au	6.46852767	1.95396552	3.23196681
Au	1.48018857	4.83146211	3.21425336
Au	3.15261395	1.94043346	5.63927833
Au	8.14584006	4.82274012	5.61527918
Au	9.82001036	1.93910772	8.13592781
Au	4.82986810	4.82612697	8.11133381
Au	2.29732174	0.50615073	0.74790418
Au	7.29244032	3.38880517	0.73751828
Au	8.96954233	0.50631961	3.22612782
Au	3.97538017	3.38786275	3.21335708
Au	5.65448614	0.50041036	5.63136651
Au	0.65334761	3.38939901	5.64053352
Au	2.32598947	0.49313384	8.12931522
Au	7.33940816	3.38216401	8.11034687
Au	4.79236190	7.71908084	0.69141436
Au	9.78670347	10.60274830	0.73343296
Au	1.46519807	7.71832194	3.18588177
Au	6.47473313	10.60509214	3.19002943
Au	8.14243074	7.72451738	5.60255363
Au	3.15172576	10.59452520	5.63210607
Au	4.81905365	7.74897800	7.94021051
Au	9.81544752	10.59172630	8.13803038

Au	7.28949392	6.27367529	0.71257481
Au	2.29496794	9.16328950	0.71414058
Au	3.96970597	6.27197754	3.17218586
Au	8.96193579	9.16262830	3.20189187
Au	0.63484899	6.27319289	5.60882103
Au	5.65908464	9.17348465	5.56778508
Au	7.34521543	6.27908173	8.03041587
Au	2.32253789	9.15748164	8.12115145
Au	9.78691665	7.71766962	0.72828034
Au	4.79432230	10.60276676	0.71912819
Au	6.46235397	7.71072786	3.17951627
Au	1.47350809	10.59892957	3.21815365
Au	3.13541841	7.71898568	5.56496554
Au	8.15056474	10.59960600	5.63851703
Au	9.81788194	7.71869914	8.13915374
Au	4.82581614	10.58779303	8.13295297
Au	2.29597841	6.27538539	0.71259769
Au	7.28990670	9.16092109	0.71121408
Au	8.95973894	6.27241923	3.19587815
Au	3.96841568	9.16313862	3.17763791
Au	5.64066005	6.25877481	5.59834562
Au	0.64782624	9.15582495	5.63460359
Au	2.30608579	6.28592464	8.02583036
Au	7.31892238	9.15216714	8.12409968
C	4.78885458	6.44814715	10.92290329
S	4.66925280	4.75797885	10.66840199
N	3.67853746	7.21020180	11.04104211
H	2.81390778	6.77934143	10.72329371
H	3.73637620	8.21403770	10.87979736
N	5.99384124	7.05071197	11.04007176
H	6.07796255	8.04539227	10.83582862
H	6.79058423	6.49298344	10.74282546

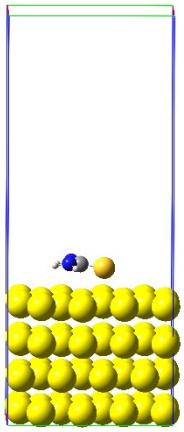

Structural Parameters of Adsorption Model with Thiourea Molecule and Pt

Tv_1:	9.611600	0.000000	0.000000
Tv_2:	0.000000	11.098500	0.000000
Tv_3:	0.000000	0.000000	29.268817
Pt	4.63416787	1.89765294	1.14907649
Pt	9.43621156	4.67089862	1.12769181
Pt	1.44830588	1.88971241	3.43081609
Pt	6.24918743	4.66196432	3.45101275
Pt	7.85104928	1.88784519	5.67019758
Pt	3.05717084	4.66234800	5.71425475
Pt	4.66070579	1.85588285	7.96301455
Pt	9.46471159	4.66037114	7.97662367
Pt	7.03984341	0.50160670	1.12514220
Pt	2.23328563	3.28536088	1.14686464
Pt	3.84340606	0.50339877	3.43176762
Pt	8.66105198	3.28343507	3.42968573
Pt	0.63950829	0.49842476	5.67471756
Pt	5.44865457	3.27919622	5.71531868
Pt	7.06703617	0.49032662	7.96614719
Pt	2.23729819	3.26458992	7.96956228
Pt	9.44061127	1.89650136	1.13824176
Pt	4.63501407	4.66991740	1.15689682
Pt	6.24919493	1.89471250	3.42906377
Pt	1.45231507	4.66676864	3.43269603
Pt	3.04331428	1.88228196	5.68544663
Pt	7.85958217	4.65566293	5.67338758
Pt	9.46502512	1.87947415	7.96844626
Pt	4.65537644	4.65850337	8.06880581
Pt	2.23399295	0.50885402	1.13953017
Pt	7.03869704	3.28282554	1.14710318
Pt	8.65004958	0.50821030	3.42355069
Pt	3.85033997	3.28061460	3.46214719
Pt	5.45076027	0.50000552	5.66895746
Pt	0.64770410	3.27605423	5.67266757
Pt	2.25055374	0.48979933	7.97200974
Pt	7.07698302	3.26331326	7.97137460
Pt	4.63348919	7.44396927	1.13503389
Pt	9.44422638	10.21867163	1.13541205
Pt	1.43866736	7.44416794	3.42230355
Pt	6.24823098	10.21671685	3.41978936
Pt	7.84770771	7.44062019	5.65247823
Pt	3.04728896	10.20825868	5.67555699
Pt	4.65929692	7.46074177	7.89435020
Pt	9.46210665	10.20158460	7.97015907

Pt	7.03715149	6.06024425	1.14093039
Pt	2.23193213	8.83035627	1.13397700
Pt	3.84469113	6.04938914	3.44509723
Pt	8.64357001	8.82658422	3.41750171
Pt	0.63504226	6.04883555	5.66228885
Pt	5.45397209	8.83096191	5.64740068
Pt	7.08650148	6.05303333	7.92867315
Pt	2.24957729	8.81869763	7.97256848
Pt	9.43993471	7.44742135	1.12770820
Pt	4.63698801	10.21882157	1.13289142
Pt	6.24230495	7.43650842	3.41436907
Pt	1.43867986	10.21511811	3.43226607
Pt	3.03272508	7.44116180	5.65866069
Pt	7.85365143	10.21287866	5.66870487
Pt	9.46346083	7.43366087	7.97367923
Pt	4.65900174	10.20185618	7.97509262
Pt	2.23097087	6.05571917	1.13938880
Pt	7.03935841	8.83840823	1.11222441
Pt	8.65472091	6.04923709	3.41910505
Pt	3.83981180	8.82813324	3.41965531
Pt	5.44518228	6.03246559	5.69166508
Pt	0.63501188	8.82222406	5.67239771
Pt	2.23402832	6.05622604	7.95222489
Pt	7.06330283	8.81586107	7.96905300
C	4.79133704	6.18816212	10.75475217
S	4.63864591	4.48042871	10.38776394
N	3.68363859	6.91638299	10.97375551
H	2.82370998	6.51680114	10.59513321
H	3.73432623	7.93251026	10.90348108
N	6.00616168	6.74051560	10.89892070
H	6.11276144	7.74663158	10.76363174
H	6.77870047	6.19428583	10.51040555

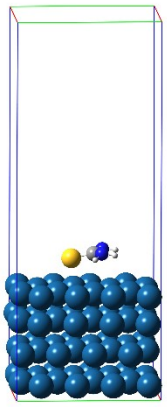

Structural Parameters of Adsorption Model with Thiourea Molecule and Pd

Tv_1:	9.530200	0.000000	0.000000
Tv_2:	0.000000	11.004600	0.000000
Tv_3:	0.000000	0.000000	31.605712
Pd	4.12192958	3.78058378	1.10812534
Pd	8.88964324	6.53182193	1.11483555
Pd	0.94397851	3.78353720	3.39981348
Pd	5.72042717	6.53667022	3.40244529
Pd	7.31012609	3.78636120	5.61544911
Pd	2.54226367	6.52973931	5.66931789
Pd	4.12262891	3.76187970	7.95766215
Pd	8.86244004	6.55862484	7.93253782
Pd	6.50592350	2.40320909	1.09086325
Pd	1.74157381	5.15627763	1.13001198
Pd	3.32737660	2.40750704	3.38333079
Pd	8.10613919	5.15882398	3.39260359
Pd	0.13630121	2.40608217	5.61604299
Pd	4.92439196	5.15980570	5.64363414
Pd	6.49835624	2.41015662	7.89697065
Pd	1.67177205	5.15640187	7.96505346
Pd	8.88732349	3.78151235	1.10381211
Pd	4.12337445	6.53142510	1.12766146
Pd	5.71357810	3.77897733	3.38586082
Pd	0.95289372	6.53101793	3.41360685
Pd	2.53340906	3.78220223	5.64219987
Pd	7.31715261	6.54276303	5.62602849
Pd	8.86004787	3.77444420	7.93425401
Pd	4.16108174	6.58588048	7.96211950
Pd	1.73950223	2.40489191	1.10782003
Pd	6.50251255	5.15549245	1.11047744
Pd	8.08804372	2.40242952	3.37186676
Pd	3.33590146	5.15664023	3.41639099
Pd	4.90616440	2.42371374	5.63233510
Pd	0.17142828	5.15706248	5.67495319
Pd	1.71347268	2.39010096	7.86587473
Pd	6.52110282	5.16739877	7.87823194
Pd	4.12654286	9.28068132	1.10946858
Pd	8.88901663	1.02846868	1.08887398
Pd	0.94741386	9.28565045	3.39226351
Pd	5.70242205	1.02584705	3.37245811
Pd	7.29272766	9.28521048	5.62814228
Pd	2.53080360	1.02676439	5.60428534
Pd	4.12641163	9.32502348	7.92982384
Pd	8.87397635	1.03570420	7.90584079

Pd	6.50855307	7.90706734	1.10803210
Pd	1.74121738	10.65737527	1.09490910
Pd	3.33745870	7.90477838	3.41292796
Pd	8.08627120	10.65904423	3.37805010
Pd	0.15735866	7.91251054	5.63656047
Pd	4.91222094	10.65993439	5.62041342
Pd	6.51757836	7.93806070	7.93285324
Pd	1.73562420	10.67562926	7.90511291
Pd	8.89233657	9.28189249	1.10133043
Pd	4.12397791	1.02886847	1.09251939
Pd	5.70960743	9.28178475	3.38995819
Pd	0.93675576	1.02927774	3.37698278
Pd	2.53744091	9.28683718	5.63295836
Pd	7.28526885	1.03416378	5.61191465
Pd	8.88500517	9.30605694	7.90890338
Pd	4.11715257	1.04103054	7.90000859
Pd	1.74378310	7.90797258	1.12866400
Pd	6.51037887	10.65588888	1.08766254
Pd	8.10071412	7.91382427	3.38902203
Pd	3.32343710	10.65604569	3.37520306
Pd	4.91661226	7.89542392	5.67351102
Pd	0.14422852	10.66263987	5.61813054
Pd	1.72838592	7.94546734	7.91999035
Pd	6.50175194	10.67924053	7.91380511
C	3.89210680	4.08710932	10.08599648
S	3.04905369	5.65555952	9.75544878
N	3.08989774	3.08267315	10.61628755
H	2.19025982	3.00235608	10.12700742
H	3.54601197	2.17051242	10.66902484
N	5.17442076	4.17140841	10.61946929
H	5.66842201	3.27772286	10.64564799
H	5.74908514	4.87524953	10.14000464

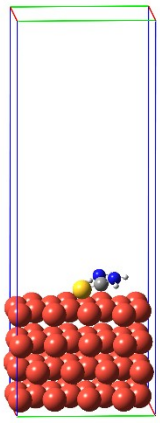

Figures

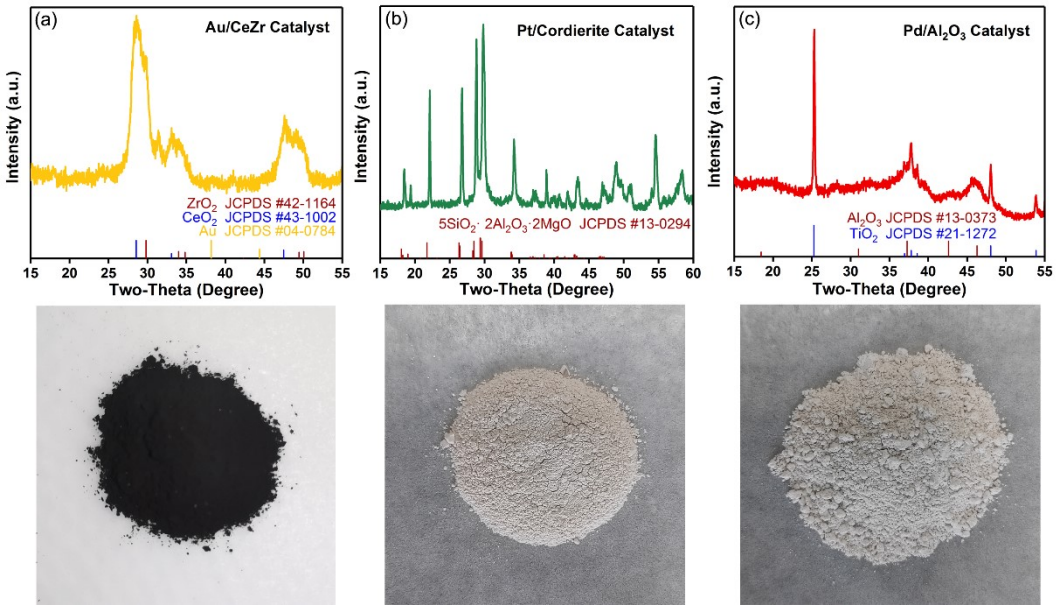

Figure S1 Original forms of PMs-containing spent catalysts. (a) Au/CeZr powder catalyst, (b) Pt/CM catalyst, and (c) Pd/Al_2O_3 spherical catalyst.

XRD analysis showed that Au/CeZr catalyst had a poor crystallization of ZrO_2 and CeO_2, and a weak peak of Au crystal could be observed. Pt/Cordierite and Pd/Al_2O_3 catalyst only showed the crystal peaks of supported materials, while the Pt and Pd were difficult to be detected due to their relatively low content. They were all used in the forms of powder.

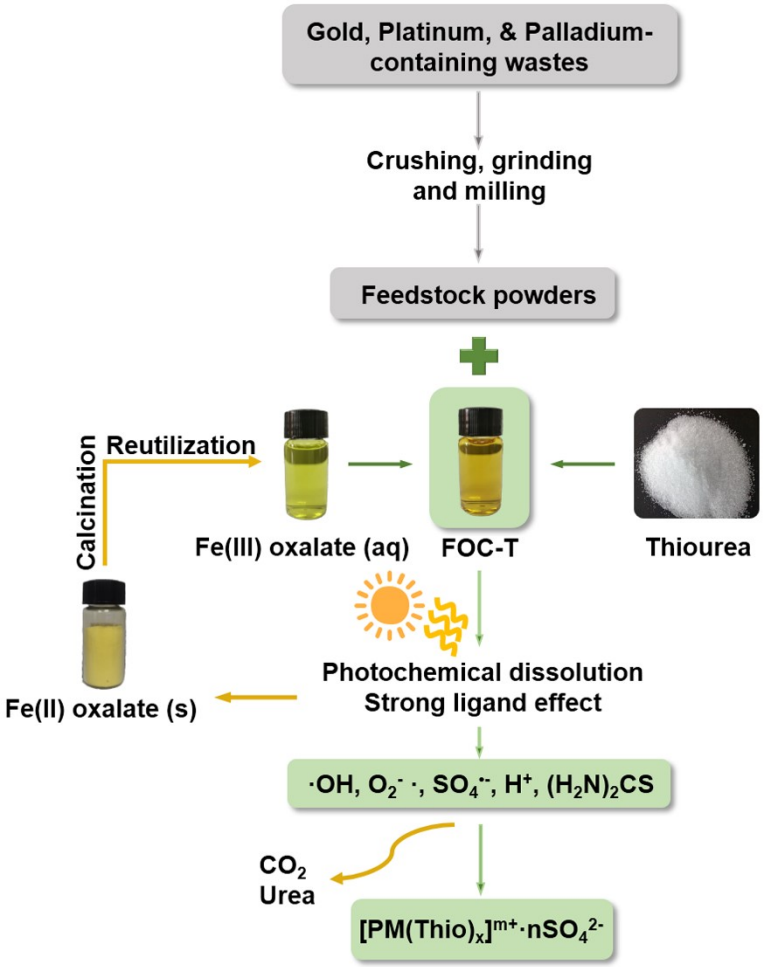

Scheme S1 Experimental flowchart of photochemical dissolution of Au, Pt, and Pd in the FOC-T system under SSL irradiation.

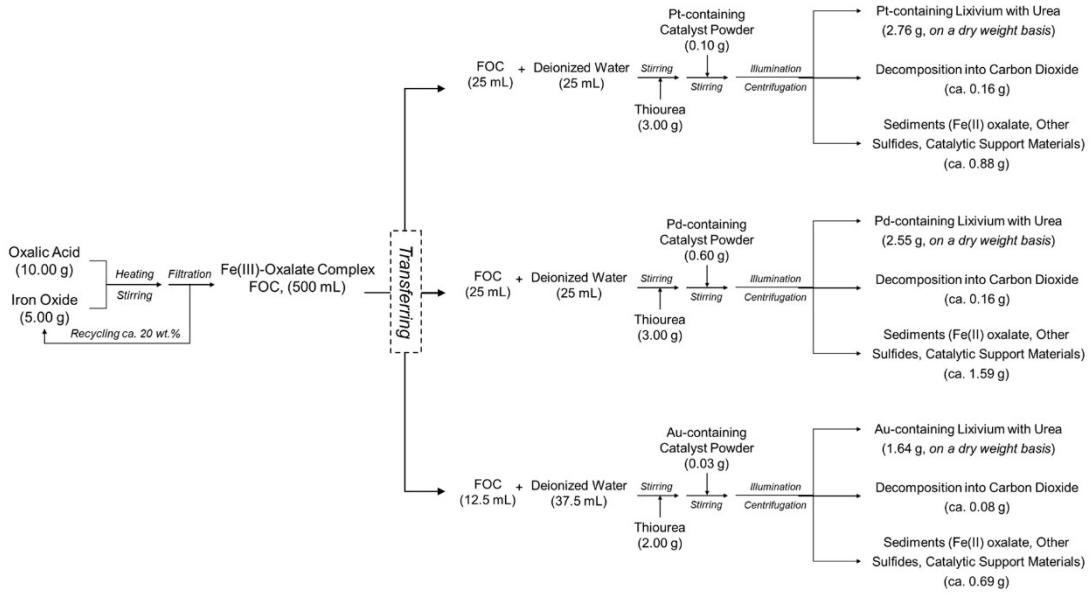

Figure S2 Pictorial flow-sheet with mass balance for Pt, Pd, and Au recovery in FOC-T system under their own optimal conditions.

In the recovery process, the lixiviant consists of Fe (III)-oxalate (FOC) and thiourea. Bulk FOC is synthesized by the oxalic acid and iron oxide with 500 mL DI water at the temperature of 98 ^{o}C, and transferred to be as a leaching agent. Then, the Pt/Pd/Au-containing catalyst powder is added into the system under their own optimal conditions including FOC addition volume ratio, thiourea concentration, solid-to-liquid ratio between catalyst powder and FOC-T lixiviant, and dissolution time. After the sufficient irradiation, Pt/Pd/Au is dissolved into liquid phase blended with urea which comes from the chemical transformation of thiourea. After separation, the Pt/Pd/Au-containing lixivium can be used as a chemical precursor.

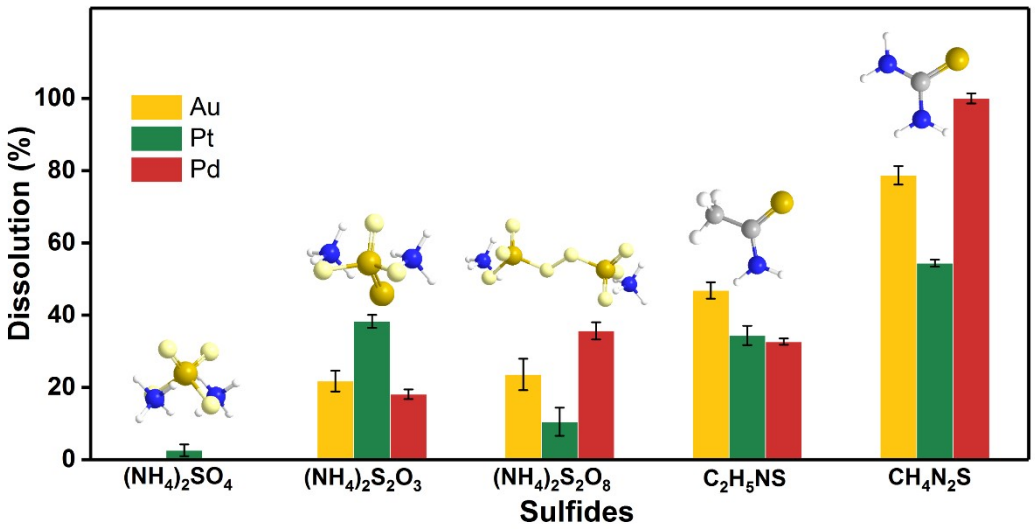

Figure S3 Common sulfides as lixiviants for PMs photochemical dissolution in Fe(III)-oxalate complexes. (0.05 mol·L^{-1} FOC, 60 g·L^{-1} sulfides, 10 g·L^{-1} Pt/CM or Pd/Al_2O_3 catalyst or 1 g·L^{-1} Au/CeZr catalyst, RT, 300 rpm/min and SSL irradiation for 4 h)

On the one hand, thiourea was chemically stable under acidic condition, and the sulfur radicals could be generated availably in photochemistry. On the contrary, thioacetamide and ammonium thiosulfate might break down into hydrogen sulfide, sulfates and other sulfur-containing materials in an acidic solution[2], and an odor similar to rotten eggs can be smelled during the experiment. This behavior would greatly reduce the recovery performance of precious metals. On the other hand, thiocarbonyl and amino groups of thiourea could reduce the surface tension of liquids[3], promoting full contact between the solution and the metal surface. These groups could strongly bind the precious metals to form stable complexes.

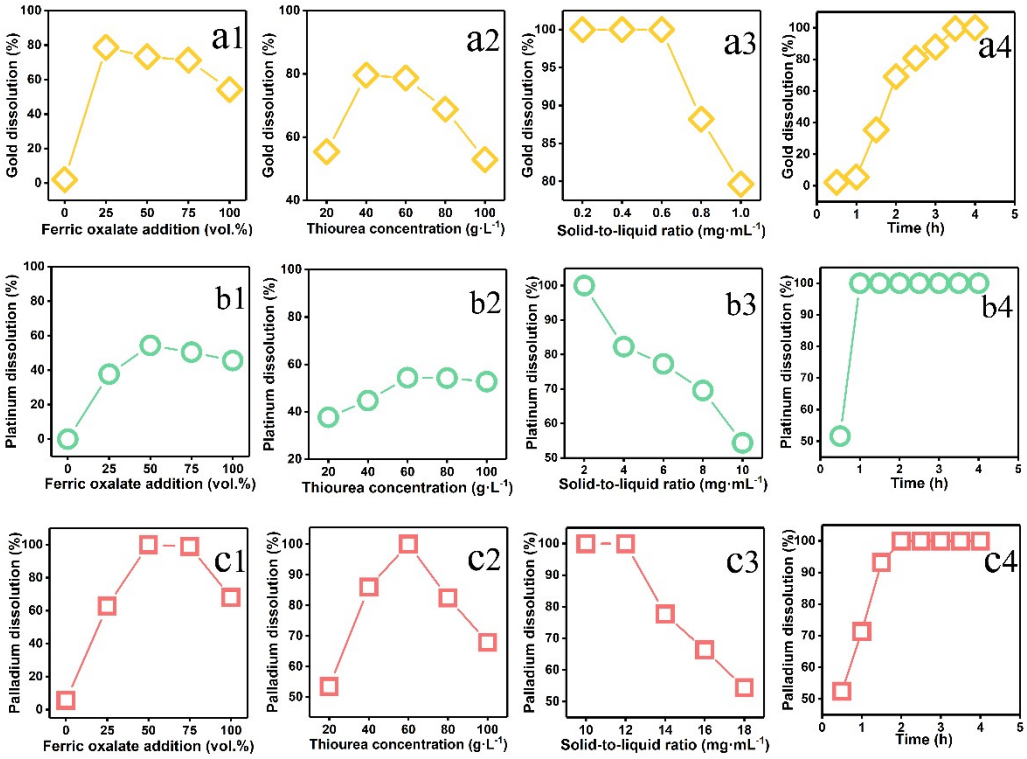

Figure S4 Factors optimization for PMs dissolution in the FOC-T system: PMs dissolution of (a) Au, (b) Pt, and (c) Pd under the conditions of (1) FOC addition, (2) thiourea concentration, (3) solid-to-liquid ratio of feedstocks, and (4) dissolution time.

The optimal conditions of PMs recovery in FOC-T system (RT, 300 rpm/min):

For Au dissolution, it was 25 vol.% FOC (0.02 mol·L^{-1}) addition, 40 g·L^{-1} thiourea concentration, 0.6 $g_{spent\ catalyst}$·L^{-1} solid-to-liquid ratio, and reaction time for 3.5 h.

For Pt dissolution, it was 50 vol.% FOC (0.05 mol·L^{-1}) addition, 60 g·L^{-1} thiourea concentration, 2 $g_{spent\ catalyst}$·L^{-1} solid-to-liquid ratio, and reaction time for 1 h.

For Pd dissolution, it was 50 vol.% FOC (0.05 mol·L^{-1}) addition, 60 g·L^{-1} thiourea concentration, 12 $g_{spent\ catalyst}$·L^{-1} solid-to-liquid ratio, and reaction time for 2 h.

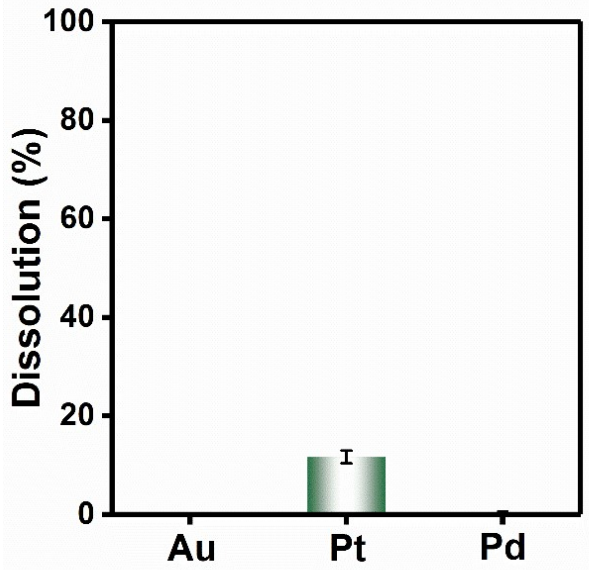

Figure S5 Photochemical dissolution performance of PMs in FOC-urea system. (0.05 mol·L^{-1} FOC vol.% FOC, 60 g·L^{-1} urea, 10 g·L^{-1} Pt/CM catalyst or 10 g·L^{-1} Pd/Al_2O_3 catalyst or 1 g·L^{-1} Au/CeZr catalyst, RT, 300 rpm/min and SSL irradiation for 4 h)

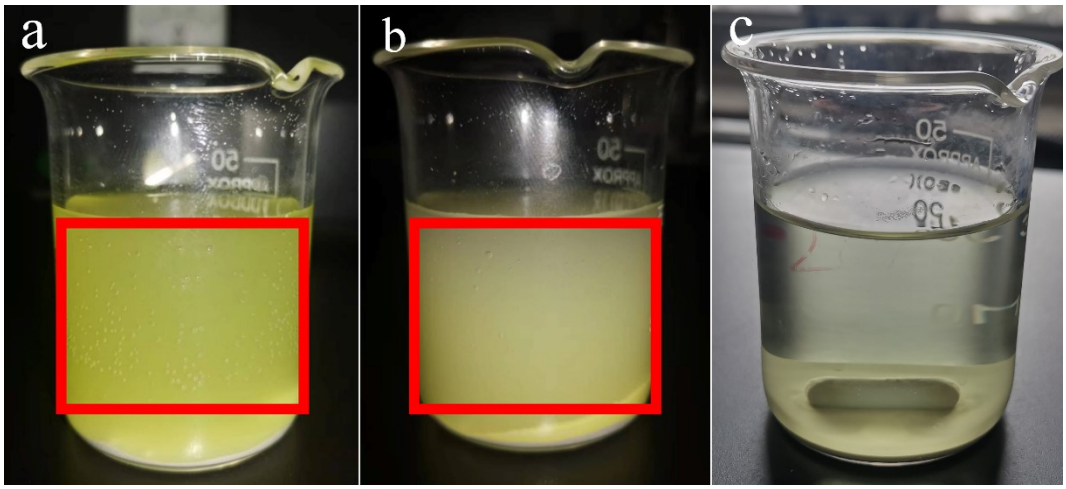

Figure S6 Record for the gas generation from the Fe(III) oxalate photo-degradation reaction mixed with spent catalyst powder: (a) reaction in the progress, (b) reaction in the end, and (c) standing treatment.

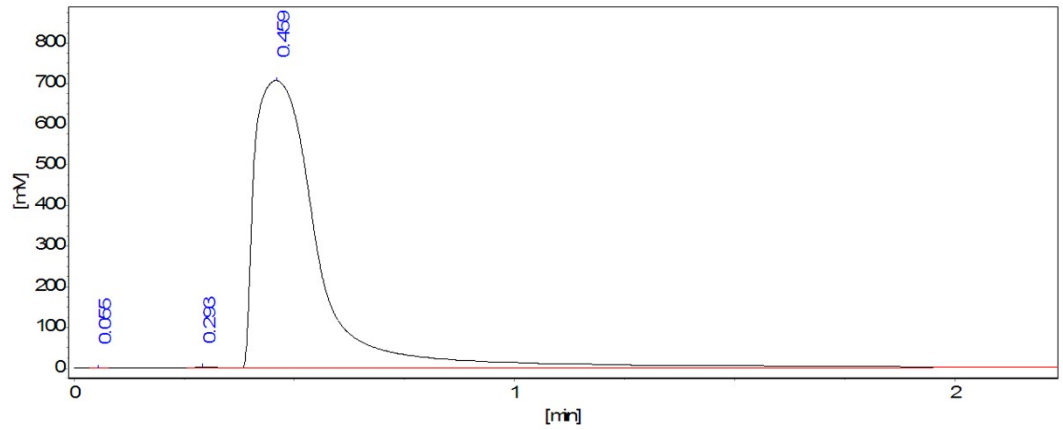

Figure S7 Gas chromatography analysis during FOC photodegradation.

The peak at 0.459 min is assigned to carbon dioxide. It indicates that the main component in the tail gas is carbon dioxide.

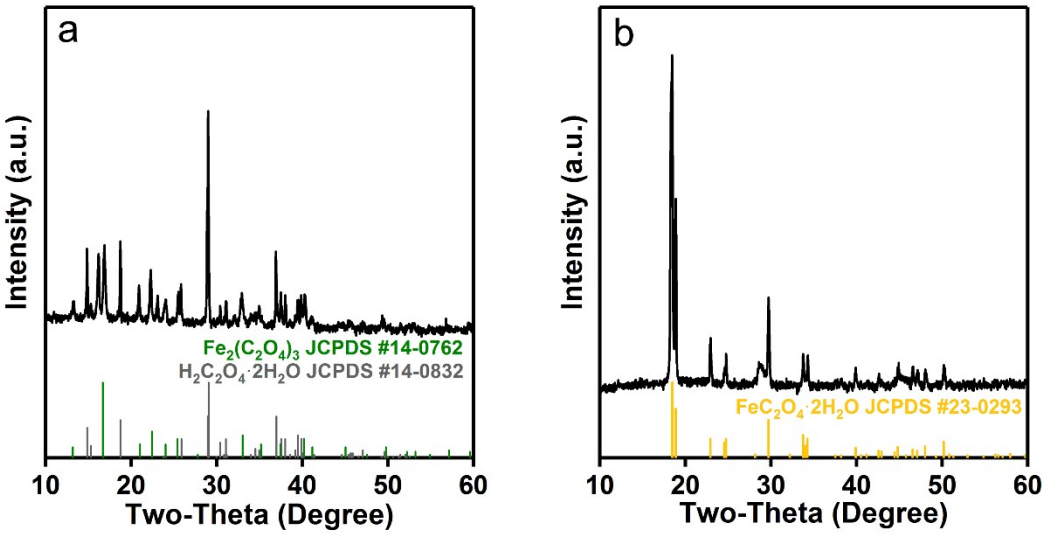

Figure S8 XRD patterns of (a) FOC and (b) the sediment after FOC photodegradation.

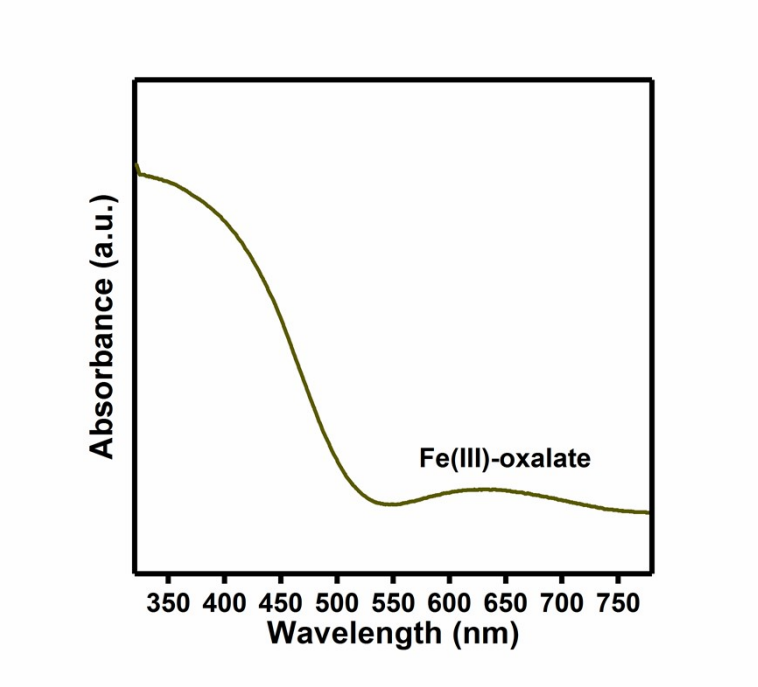

Figure S9 UV-vis spectroscopy of FOC.

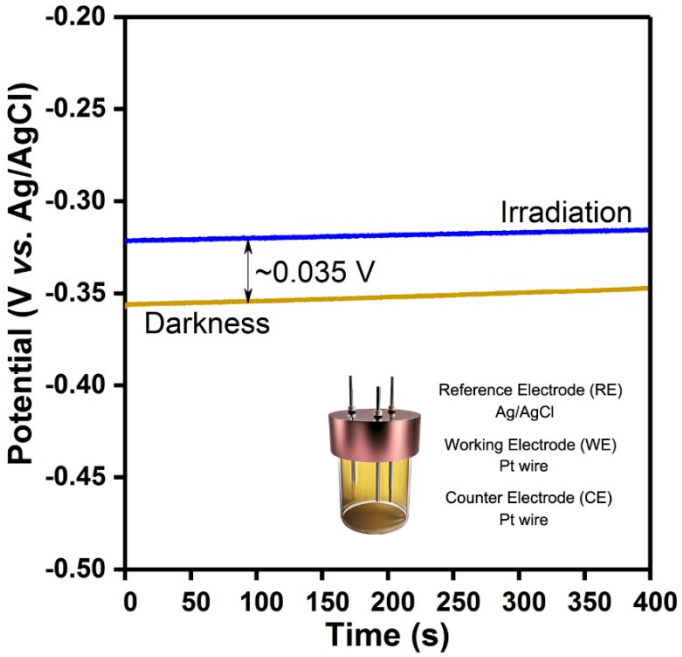

Figure S10 Open circuit potential curves of the FOC-T lixiviant in darkness and under irradiation.

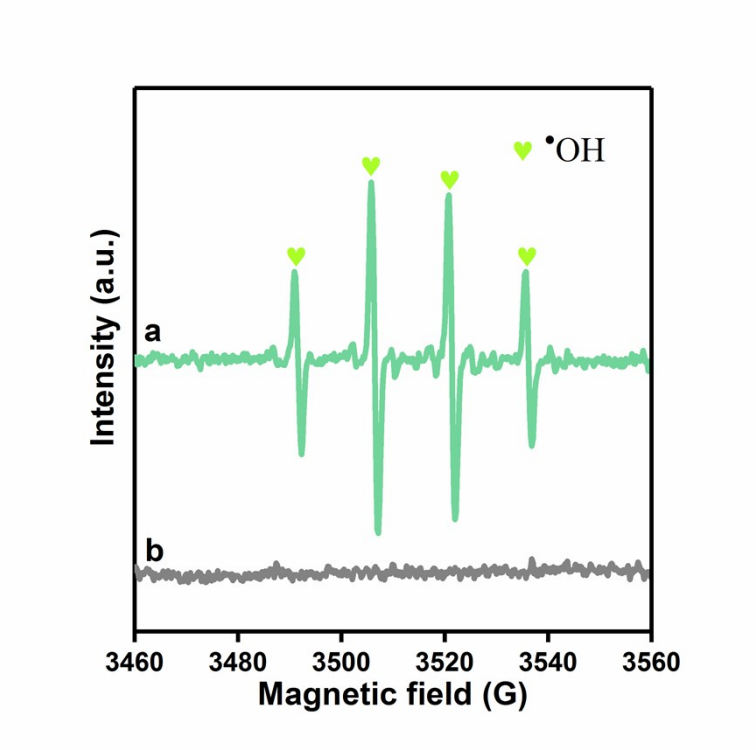

Figure S11 EPR spectra of DMPO-radical adduct with irradiation for 30 min in (a) bare FOC system and (b) bare thiourea system.

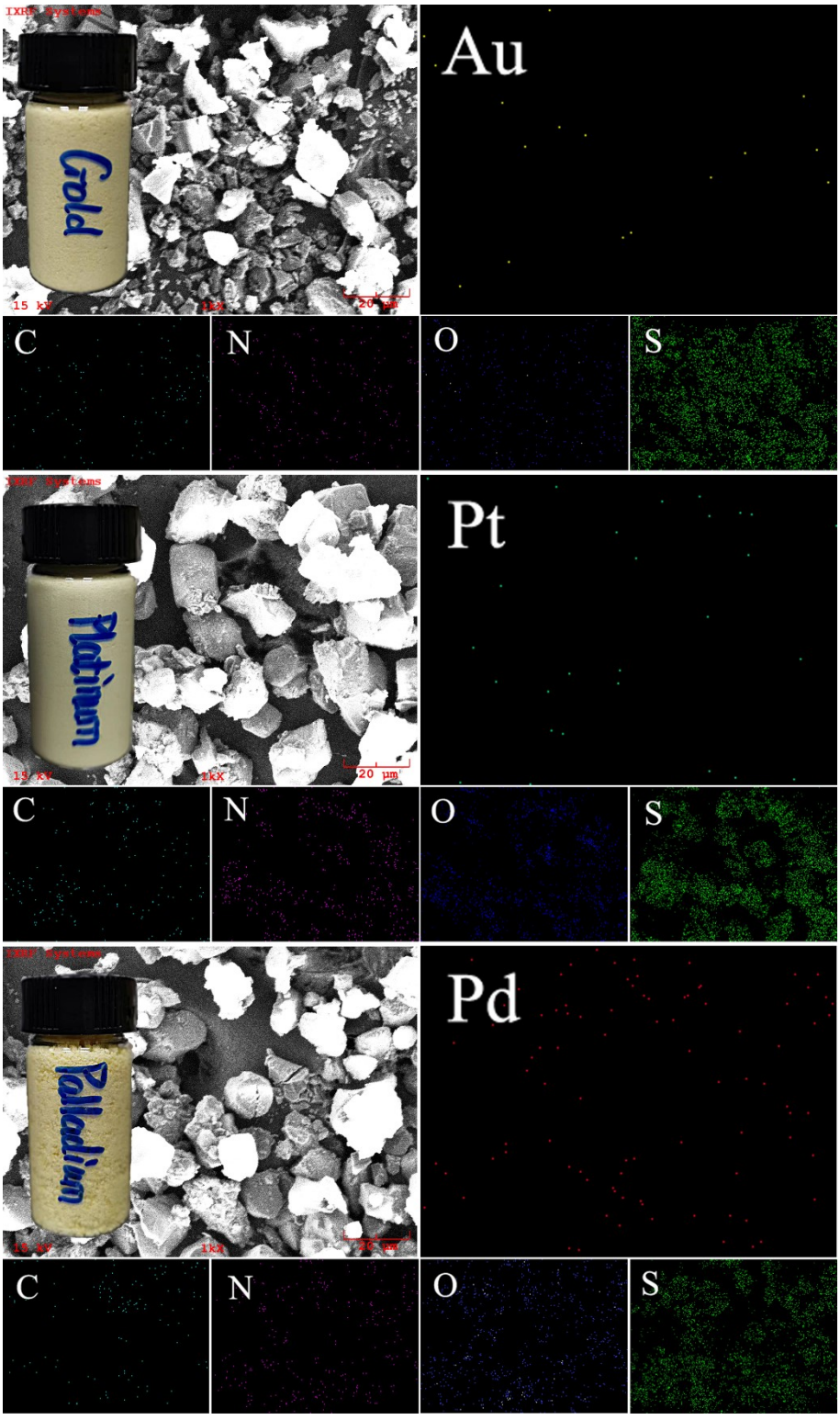

Figure S12 SEM-EDX analysis of Au(Thio), Pt(Thio), and Pd(Thio).

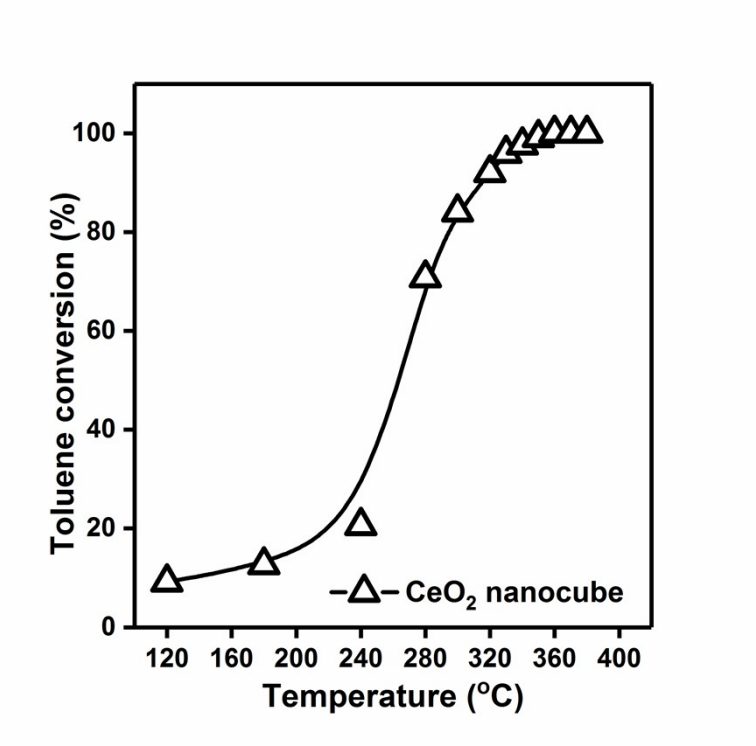

Figure S13 Catalytic performance of CeO_2 catalysts for toluene oxidation.

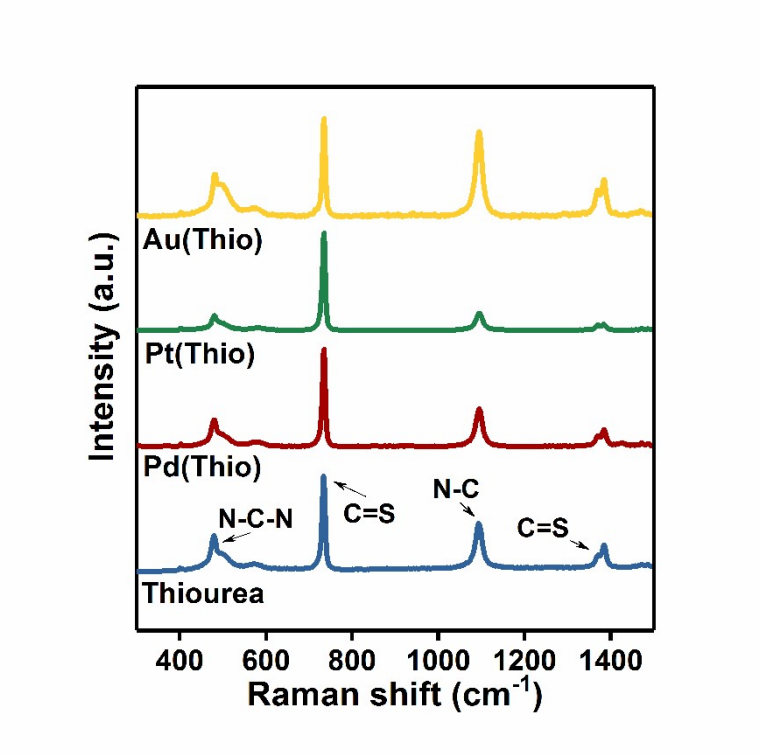

Figure S14 Raman spectra of Au(Thio), Pt(Thio), Pd(Thio), and thiourea.

Two signal peaks at 730 and 1380 cm^{-1} were assigned to the C=S stretching vibration, and those at 479 and 1094 cm-1 was corresponding to the bending and stretching vibration of N-C=S.[4]

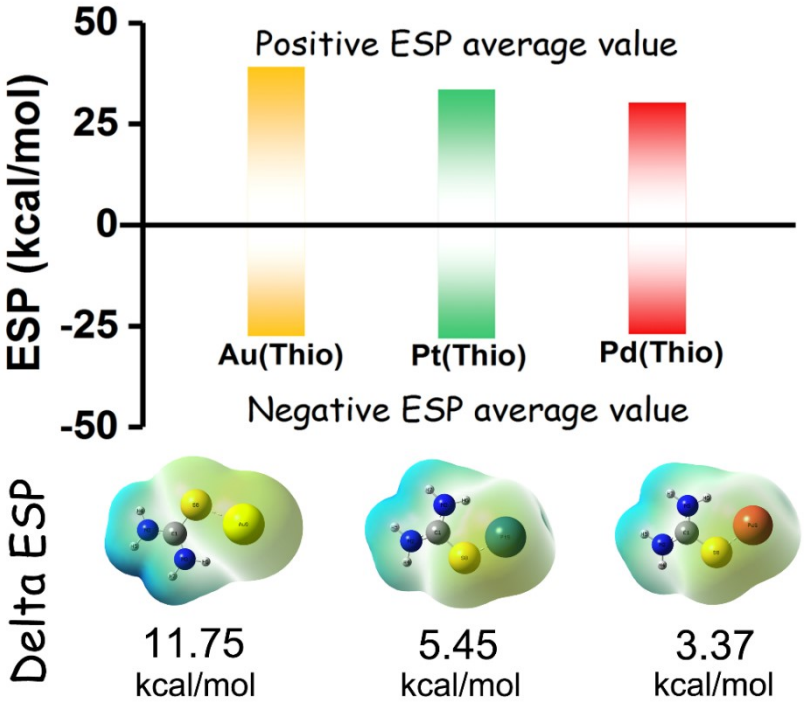

Figure S15 Computational ESP mapped over the electron density isosurface of PMs(Thio) complexes.

Tables

Table S1 Chemical compositions of the support for Pt/CM catalyst (wt%)

Al_2O_3	TiO_2	MgO	CaO	SiO_2	CeO_2	Fe_2O_3	La_2O_3	SO_3	K_2O	P_2O_5
31.63	0.52	13.26	1.00	50.19	1.93	0.64	0.36	0.04	0.16	0.09

Table S2 Chemical compositions of the support for Pd/Al_2O_3 catalyst (wt%)

Al_2O_3	TiO_2	Na_2O	CaO	SiO_2	SO_3	Fe_2O_3
92.72	6.65	0.36	0.09	0.08	0.04	0.04

Table S3 PMs dissolution performance under different dissolution conditions

NO.	Lixiviant composition	Illumination	Dissolution efficiency
1	Fe(III) oxalate	No	Au: 0 % Pt: 0 % Pd: 0 %
2	Fe(III) oxalate	Yes	Au: 0 % Pt: 0 % Pd: 0 %
3	Thiourea	No	Au: 14.66 % Pt: 0 % Pd: 1.19 %
4	Thiourea	Yes	Au: 14.74 % Pt: 0 % Pd: 3.29 %
5	Fe(III) oxalate & Thiourea	No	Au: 11.82 % Pt: 0 % Pd: 30.39 %
6	Fe(III) oxalate & Thiourea	Yes	Au: 99.55 % Pt: 100 % Pd: 100 %

Table S4 Current studies about PMs recovery via photochemical oxidization reactions

Precious Metals	Radical sources	Solution	Reactive species	Illuminant	Temp. /°C	Hazardous risk	Ref.
Au, Ag, Pt, Pd, Ru, Rh, Ir	TiO_2	Acetonitrile, Dichloromethane	h^+, e^-, ·OH, $\cdot O_2^-$, $CH_2CN^\bullet$, $CHCl_2^\bullet$	100 W ultraviolet LED lamp	RT	Yes	Chen et al.[5]
Au, Pt	TiO_2	Acetonitrile, Dichloromethane	h^+, e^-,·OH, $\cdot O_2^-$, $CN^\bullet$, $Cl^\bullet$	100 W ultraviolet LED lamp	RT	Yes	Chen et al.[6]
Au, Pd	TiO_2	NH_4Br, NH_4I	h^+, e^-, ·OH, $\cdot O_2^-$	100 W ultraviolet LED lamp	RT	No	Cao et al.[7]
Au, Pt, Pd, Ru, Rh, Ir	P-TiO_2	Acetonitrile, Dichloromethane	h^+, e^-, ·OH, $\cdot O_2^-$, $CH_2CN^\bullet$, $CHCl_2^\bullet$	100 W ultraviolet LED lamp	RT	Yes	Qiao et al.[8]
Au, Pt	CeO_2	Acetonitrile, Dichloromethane	h^+, e^-,·OH, $\cdot O_2^-$, $CH_2CN^\bullet$, $CHCl_2^\bullet$	100 W ultraviolet LED lamp	RT	Yes	Chen et al.[9]
Au	TiO_2	Acetonitrile, NaOH	h^+, e^-,·OH, $\cdot O_2^-$, $CH_2CN^\bullet$, $CN^\bullet$	100 W ultraviolet LED lamp	RT	Yes	Shang et al.[10]
Au	Benzaldehyde, Benzylalcohol	Acetonitrile	·OH, $CH_2CN^\bullet$, $CN^\bullet$	300 W high-pressure mercury lamp	RT	Yes	Li et al.[11]
Au, Pd	Peroxydisulfate	NaCl	·OH, $SO_4^{-}\cdot$	50 W Xe lamp	60	No	Ding et al.[12]
Pt, Pd	Fe(III) oxalate	NaCl	·OH, $\cdot O_2^-$	85W ultraviolet LED lamp/sunlight	RT	No	Zhao et al.[13]
Au, Pt, Pd	Fe(III) oxalate	Thiourea	·OH, $\cdot O_2^-$, $SO_4^{-}\cdot$	500 W Xe lamp	RT	No	This work

Table S5 Economic benefit estimation of recovery of per gram precious metal in comparison with commercial chlorinated compounds

Precious Metals	**Purchase Cost** [a]	**Fe(III)-oxalate Cost** [b]	**Thiourea Cost** [b]	**Commercial Price/$** [c]
Gold	**$** 40.00	**$** 0.63	**$** 10.02	108.16
Total Cost/$		**50.65**		**Value/$** **+57.51**
Platinum	**$** 47.60	**$** 6.25	**$** 75.02	156.12
Total Cost/$		**128.87**		**Value/$** **+27.25**
Palladium	**$** 134.40	**$** 1.50	**$** 18.00	206.01
Total Cost/$		**153.90**		**Value/$** **+52.11**

[a] The purchase prices of spent precious metal-containing catalyst are determined by market quotation.

[b] The dosages of Fe(III)-oxalate and thiourea are in line with the optimal conditions of PMs dissolution.

c The commercial prices of chlorinated compounds comes from *Aladdin Chemical Reagent Co., Ltd.*

$HAuCl_4$ CAS: 16961-25-4; H_2PtCl_6 CAS: 16941-12-1; $(NH_4)_2PdCl_4$ CAS: 13820-40-1.

Reference

1. Ren, J.; Zhang, Z.; Chen, Z.; Wan, L.; Shi, K.; Zeng, X.; Li, J.; Liu, Q., Interfacial process engineering of a co-grinding agent for recycling spent lithium-ion batteries. *Green Chemistry* **2023,** 25**,** 9795-9804.
2. Mandal, G. C.; Saikh, F.; Ray, S. K.; Pramanik, K.; Giri, L., Eliminating H_2S and any sulfide reagents from qualitative inorganic analysis: An ultimate solution to a long-standing problem. *Journal of Chemical Education* **2024**, 101, 10, 4468–4471.
3. Mousavi, N. S.; Vaferi, B.; Romero-Martinez, A., Prediction of surface tension of various aqueous amine solutions using the UNIFAC model and artificial neural networks. *Industrial & Engineering Chemistry Research* **2021**, 60, 28, 10354–10364.
3. Sun, H.; Wang, H.; Qu Z., Construction of CuO/CeO_2 catalysts via the ceria shape effect for selective catalytic oxidation of ammonia. *ACS Catalysis* **2023**, 13, 1077−1088.
4. Kumari, R. G.; Ramakrishnan, V.; Carolin, M. L.; Kumar, J.; Sarua, A.; Kuball, M., Raman spectral investigation of thiourea complexes. *Spectrochim. Acta A* **2009,** *73*, (2), 263-267.
5. Chen, Y.; Xu, M.; Wen, J.; Wan, Y.; Zhao, Q.; Cao, X.; Ding, Y.; Wang, Z. L.; Li, H.; Bian, Z., Selective recovery of precious metals through photocatalysis. *Nature Sustainability* **2021,** *4*, (7), 618-626.
6. Chen, Y.; Guan, S.; Ge, H.; Chen, X.; Xu, Z.; Yue, Y.; Yamashita, H.; Yu, H.; Li, H.; Bian, Z., Photocatalytic dissolution of precious metals by TiO_2 through photogenerated free radicals. *Angewandte Chemie International Edition* **2022**, *61*, e202213640.
7. Cao, J.; Chen, Y.; Shang, H.; Chen, X.; Qiao, Q.; Li, H.; Bian, Z., Aqueous photocatalytic recycling of gold and palladium from waste electronics and catalysts. *ACS ES&T Engineering* **2022,** *2*, (8), 1445-1453.
8. Qiao, Q., Chen, Y., Wang, Y., Ren, Y., Cao, J., Huang, F., Bian, Z., Surface modification of phosphate ion to promote photocatalytic recovery of precious metals. *Chinese Chemical Letters* **2023**, *34*, 107394.
9. Chen, Y.; He, H.; Xu, S.; Zou, Z.; Hua, W.; Bian, Z.; Li, H.; Yue, Y., Precious metal catalyst recycling through photocatalytic dissolution. *Green Chemistry* **2023,** *25*, (19), 7518-7523.
10. Shang, H., Chen, Y, Guan, S., Wang, Y., Cao, J., Wang, X., Li, H., Bian, Z., Scalable and selective gold recovery from end-of-life electronics. *Nature Chemical Engineering* **2024**, 1, 170–179.
11. Li, R.; Kobayashi, H.; Tong, J.; Yan, X.; Tang, Y.; Zou, S.; Jin, J.; Yi, W.; Fan, J., Radical-involved photosynthesis of AuCN oligomers from Au nanoparticles and acetonitrile. *Journal of the American Chemical Society* **2012,** *134*, (44), 18286-18294.
12. Ding, A., Li, M., Liu, C., Chee, T-S., Yan, Q., Lei, L., Xiao, C., Recovering palladium and gold by peroxydisulfate-based advanced oxidation process. *Science Advances* **2024**, *10*, (21), eadm9311.
13. Zhao, X.; Liang, G.; Wang, H.; Qu, Z., New insight toward synergetic effect for platinum recovery coupling with Fe(III)-oxalate complexes degradation through photocatalysis. *ACS Sustainable Chemistry & Engineering* **2023,** *11*, (31), 11580-11589.